(2)

NASA
Technical Memorandum 104342

AVSCOM
Technical Report 90-C-031

A System-Approach to the Elastohydrodynamic Lubrication Point-Contact Problem

Sang Gyu Lim
Lewis Research Center
Cleveland, Ohio

and

David E. Brewe
Propulsion Directorate
U.S. Army Aviation Systems Command
Lewis Research Center
Cleveland, Ohio

Prepared for the
Annual Meeting of the Society of Tribologists and
Lubrication Engineers
Montreal, Quebec, Canada, April 29-May 2, 1991

NASA

A SYSTEM-APPROACH TO THE ELASTOHYDRODYNAMIC LUBRICATION POINT-CONTACT PROBLEM

Sang Gyu Lim*
National Aeronautics and Space Administration
Lewis Research Center
Cleveland, Ohio 44135

and

David E. Brewe
Propulsion Directorate
U.S. Army Aviation Systems Command
NASA Lewis Research Center
Cleveland, Ohio 44135

SUMMARY

The classical EHL point contact problem is solved using a new "system-approach," similar to that introduced by Houpert and Hamrock for the line-contact problem. Introducing a body-fitted coordinate system, the troublesome free-boundary is transformed to a fixed domain. The Newton-Raphson method can then be used to determine the pressure distribution and the cavitation boundary subject to the Reynolds boundary condition. This method provides an efficient and rigorous way of solving the EHL point contact problem with the aid of a supercomputer and a promising method to deal with the transient EHL point contact problem. A typical pressure distribution and film thickness profile are presented and the minimum film thicknesses are compared with the solution of Hamrock and Dowson. The details of the cavitation boundaries for various operating parameters are discussed.

E-6116

NOMENCLATURE

a,b	semi-major and semi-minor axes of contact ellipse, m
E	The Young modulus of elasticity, Pa
E′	equivalent elastic constant, Pa $\frac{2}{E'} = \frac{(1-\nu_A^2)}{E_A} + \frac{(1-\nu_B^2)}{E_B}$
f	normal force, N
G	dimensionless material parameter, $\alpha E'$
$\hat{G}$	dimensionless cavitation boundary
$\hat{g}$	cavitation boundary function
H	dimensionless film thickness

*National Research Council-NASA Research Associate at Lewis Research Center.

H_{min} dimensionless minimum film thickness

H_0 dimensionless reference film thickness

h film thickness, m

h_{min} minimum film thickness, m

h_0 reference film thickness, m

k ellipticity parameter

$\hat{n}$ normal direction

P dimensionless pressure

P_0 Roelands pressure-viscosity constant, 1,96e8 Pa

p pressure, Pa

p_h Hertzian pressure, Pa

u_m mean entraining velocity, m/s

x,y cartesian coordinates

INTRODUCTION

In the design of nonconformal contact machine elements, knowledge of elasto-hydrodynamic lubrication (EHL) is needed. Since the 1970's, several authors have presented their results of the point-contact EHL problem. Among them, the following Hamrock and Dowson (H.D.) formula (ref. 1) is widely used in the design of many machine elements:

$$(H_{min})_{H.D.} = 3.63U^{0.68}G^{0.49}W^{-0.073}(1 - e^{0.68k}) \quad (1)$$

For an EHL solution, a nonlinear integro-differential equation must be solved, the Reynolds equation and the elasticity equation. The nonlinearities are due to: (1) the dependence of the lubricant properties, (viscosity and density), on the pressure; (2) the dependence of the film thickness on the pressure; and (3) the free boundary at the exit region. Even for the hydrodynamic lubrication, since the free boundary is dependent on the pressure distribution, the Reynolds equation has non-linear characteristics. It is well known to computational lubrication engineers that the numerical treatment of the point-contact EHL problem has inherent difficulties. One can see how difficulties arise upon careful consideration of the above mentioned nonlinearities. For example, one of the major difficulties is the piezoviscous effect. At high loads the viscosity of the fluid can vary by 10 orders of magnitude within the conjunction, which caused the pressure spikes and numerical difficulties.

Another difficulty associated with solving the EHL point-contact case is to locate the free boundary where cavitation occurs. In the solution presented by H.D. Christopherson's method (ref. 2) was used together with a Gauss-Seidel iterative scheme. The essence of this method is to truncate the negative pressures as they occur during iteration and the outlet boundary is located automatically. Oh and Rhode (ref. 7) solved the point contact EHL problem using a finite element method and Newton's method. But, it has been found that the nonnegativity condition was needed

Newton's method. But, it has been found that the nonnegativity condition was needed to be checked in each iteration and the discrimination between the continuous film region and the cavitated region was troublesome. Though the solution can be obtained it is unavoidable that the solution is dependent upon the mesh size distribution near the boundary.

Finally, the large amount of computation time and computer memory space are concerns in this calculation. The majority of CPU time is devoted to the calculation of the elastic deformation. In general, the Gauss-Seidel iterative method requires more than one hundred times of iterations to obtain the converged solution. Furthermore, to obtain a solution for a given load, one additional loop is required to find the reference film thickness.

This all adds up to the fact that it is very difficult to achieve a stable solution at relatively high loads and short CPU times. Recognizing this, Houpert and Hamrock (ref. 8) devised an elegant scheme for the line contact case that enabled higher load calculations and saved on computational time as well. This scheme was an adaptation of Okamura (ref. 9) and became known as the "system approach." Using a Newton-Raphson algorithm, the pressures, the integration constant, and the reference film thickness are found simultaneously. Here advantage has been taken of the fact that the one-dimensional Reynolds equation can be integrated analytically to obtain dp/dx and in turn used with the Reynolds' boundary conditions to locate the cavitation boundary.

To the author's knowledge, the system-approach has not been successfully applied to the point-contact problem. Unlike the line-contact case, the two dimensional Reynolds equation can not be integrated analytically. However, a successful formulation of the system-approach can nevertheless be accomplished by introducing a body-fitted coordinate system and transforming the unknown physical boundary into a fixed computational boundary. The unknown boundary function becomes a part of the system matrix. In addition, the reference film thickness can be calculated simultaneously as was done in the line-contact case. This reduces the number of visits to the elastic deformation subroutine substantially. However, as was pointed out by Lubrecht et al., (ref. 3), computer memory may be a problem since the Jacobian matrix is a full matrix due to the elasticity equation. This problem can be overcome by using the block tridiagonal approximation of the system matrix. The matrix inversion is accomplished by the Thomas algorithm, and there is no need to store the whole Jacobian matrix. Furthermore, the force-balance loop can be obviated by including it in the system equations and solving simultaneously.

In this paper, the classical EHL point-contact problem is revisited with a new formulation: a free boundary value problem using the system-approach described above. The minimum film thicknesses are compared with equation (1) and the details of the free boundary are discussed.

2. ANALYTIC FORMULATION

2.1 Contact Geometry

Figure 1 shows the physical model of the elliptical contact, where the x-axis represents the rolling or sliding direction, x_A and y_B are the inlet boundaries and $x = \hat{g}(y)$ is the outlet or cavitation boundary. The ellipticity parameter is expressed in terms of the curvature difference (T), the elliptic integral of the first (F), and the second kind (S) as

$$k = \sqrt{\frac{2F - S(1 + T)}{S(1 - T)}} \tag{2}$$

where

$$F = \int_0^{\pi/2} \left\{ 1 - \left[1 - \frac{1}{k^2} \right] \sin^2\phi \right\}^{-1/2} d\phi$$

$$S = \int_0^{\pi/2} \left\{ 1 - \left[1 - \frac{1}{k^2} \right] \sin^2\phi \right\}^{1/2} d\phi$$

$$T = R\left[\frac{1}{R_x} - \frac{1}{R_y} \right]$$

Defining r as R_y/R_x, equation (2) can be rewritten as

$$k = \left[(r + 1) \frac{F}{S} - r \right]^{1/2} \tag{3}$$

Therefore, given r, the ellipticity parameter can be calculated iteratively.

2.2 Governing Equations

Assuming isothermal conditions and that the lubricant is Newtonian, the steady-state Reynolds equation for the point contact problem is

$$\frac{\partial}{\partial x}\left(\frac{\rho h^3}{\mu} \frac{\partial p}{\partial x} \right) + \frac{\partial}{\partial y}\left(\frac{\rho h^3}{\mu} \frac{\partial p}{\partial y} \right) = 12 u_m \frac{\partial (\rho h)}{\partial x} \tag{4}$$

and, using the parabolic approximation for the geometry, the film thickness is expressed by

$$h(x,y) = h_0 + \frac{x^2}{2R_x} + \frac{y^2}{2R_y} + \frac{2}{\pi E'} \int\int_\Omega \frac{p(x',y')dx'dy'}{\sqrt{(x - x')^2 + (y - y')^2}} \tag{5}$$

The applied normal force may be balanced by the generated hydrodynamic pressure distribution,

$$f = \int\int_\Omega p(x,y)dx\,dy \tag{6}$$

Applying the Reynolds boundary condition and symmetry condition at the x-axis, the boundary conditions are:

$$\begin{aligned} &p = 0 \quad \text{at} \quad x = x_A;\ 0 \le y \le y_B, \\ &p = 0 \quad \text{at} \quad x_A = \le x \le \hat{g}(y_B);\ y = y_B, \\ p = 0;\ &\frac{\partial p}{\partial \hat{n}} = 0 \quad \text{at} \quad x = \hat{g}(y);\ 0 \le y \le y_B, \\ &\frac{\partial p}{\partial y} = 0 \quad \text{at} \quad x_A \le x \le \hat{g}(0);\ y = 0. \end{aligned} \tag{7}$$

The viscosity-pressure relation is modeled by the Roelands (11) equation, i.e.,

$$\mu = \mu_0 \exp\left\{\frac{p_o\alpha}{z}\left[\left(1 + \frac{p}{p_0}\right)^z - 1\right]\right\} \tag{8}$$

$$\alpha = \frac{z}{p_0}(\ln \mu_0 + 9.67) \tag{9}$$

and, the Dowson-Higginson relation (12) is used for the density-pressure relation,

$$\rho = \rho_0 \frac{0.59\text{x}10^9 + 1.34p}{0.59\text{x}10^9 + p} \quad p \text{ in Pa} \tag{10}$$

2.3 The Dimensionless Equations

Letting

$$P = \frac{p}{p_h},\ H = \frac{hR_x}{b^2},\ X = \frac{x}{b},\ Y = \frac{y}{a},\ \hat{G} = \frac{\hat{g}}{b}$$

$$\bar{\alpha} = \alpha p_h,\ p_h = \frac{3f}{2\pi ab},\ \bar{\mu} = \frac{\mu}{\mu_0},\ \bar{\rho} = \frac{\rho}{\rho_0}$$

the equations (4) to (6) become

$$\frac{\partial}{\partial X}\left(\frac{\bar{\rho}H^3}{\bar{\mu}}\frac{\partial P}{\partial X}\right) + \frac{1}{k^2}\frac{\partial}{\partial Y}\left(\frac{\bar{\rho}H^3}{\bar{\mu}}\frac{\partial P}{\partial Y}\right) = \lambda \frac{\partial}{\partial X}(\bar{\rho}H) \tag{11}$$

$$H(X,Y) = H_0 + \frac{1}{2}\left(X^2 + c_1Y^2\right) + \frac{2c_2}{\pi^2}\int\int_\Omega \frac{P(X',Y')dX'\,dY'}{\sqrt{(X - X')^2 + k^2(Y - Y')^2}} \tag{12}$$

$$\int\int_\Omega P(X,Y)dX\,dY = \frac{2\pi}{3} \tag{13}$$

where, $\lambda = \dfrac{12\mu_0 u_m R_x^2}{b^3 p_h}$, $c_1 = \dfrac{k^2}{r}$, $c_2 = \dfrac{k\pi p_h R_x}{E'b}$

The dimensionless parameters used here can be related to those used by Hamrock and Dowson as follows,

$$\lambda = \frac{8\pi U k^2}{W}\left(\frac{R_x}{a}\right)$$

$$\bar{\alpha} = \frac{3GWk}{2\pi}\left(\frac{R_x}{a}\right)^2$$

$$c_2 = \frac{k\pi(1+r)}{4Sr} \tag{14}$$

$$\frac{a}{R_x} = \left\{\frac{6Wk^2S}{\pi}\frac{r}{1+r}\right\}^{1/3}$$

when $K = 1$ (circular contact), c_1 and c_2 are 1.

2.4 Coordinate Transformation

Introducing the body-fitted coordinate system described in reference 13,

$$\xi = \frac{Y_B(X - X_A)}{\hat{G} - X_A}$$

$$\eta = Y \tag{15}$$

the following equations are obtained:

The Reynolds equation

$$L_1(P,\hat{G},H_0) = \frac{Y_B^2}{(\hat{G}-X_A)^2}\frac{\partial}{\partial\xi}\left(q\frac{\partial P}{\partial\xi}\right) + \frac{1}{k^2}\frac{\partial}{\partial\eta}\left(q\frac{\partial P}{\partial\eta}\right) - \frac{\xi}{k^2}\frac{\partial}{\partial\eta}\left(q\frac{\hat{G}'}{\hat{G}-X_A}\frac{\partial P}{\partial\xi}\right)$$

$$- \frac{\xi\hat{G}'}{k^2(\hat{G}-X_A)}\frac{\partial}{\partial\xi}\left(q\frac{\partial P}{\partial\eta}\right) + \frac{\xi(\hat{G}')^2}{k^2(\hat{G}-X_A)^2}\frac{\partial}{\partial\xi}\left(q\xi\frac{\partial P}{\partial\xi}\right) - \lambda\frac{Y_B}{\hat{G}-X_A}\frac{\partial}{\partial\xi}(\bar{\rho}H) = 0 \tag{16}$$

where, $\hat{G}'$ represents $d\hat{G}/dY$.
The film thickness equation

$$H(\xi,\eta) = H_0 + \frac{1}{2}\left\{\left[\frac{\xi(\hat{G}-X_A)}{Y_B} + X_A\right]^2 + c_1\eta^2\right\} + \frac{2c_2}{\pi^2}D(P,\hat{G}) \tag{17}$$

The D represents an integral operator which calculates the elastic deformation of two solids in contact resulting from the pressure distribution in the fluid film

region (Ω). In this paper, the technique presented by Chang (ref. 14) is used. This method provides and efficient way of evaluating D without lengthy and complex mathematical expressions. Since the coordinate transformation can easily be implemented to this method, the details of the algorithm are not presented here.

The force balance equation is

$$L_2(P,\hat{G}) = 2\int_0^{Y_B}\int_0^{Y_B} P\,(\xi,\eta)\,\frac{\hat{G} - X_A}{Y_B}\,d\xi\,d\eta - \frac{2\pi}{3} = 0 \tag{18}$$

In the above formulation, L_1 is the nonlinear partial differential operator and L_2 is integral operator.

3. NUMERICAL METHOD

3.1 Spatial Discretization

To provide a small mesh size near the pressure spike region, an interior stretching function (ref. 15) is adopted along the ξ-axis. The finite difference representation of the transformed Reynolds equation is provided in the appendix.

3.2 Newton's Method

The system equations are

$$L_1(P,\hat{G},H_0) = 0$$

$$L_2(P,\hat{G}) = 0 \tag{19}$$

In reference 13, for hydrodynamic case, L_1 has been solved using the Thomas algorithm to find P and $\hat{G}$, and L_2 was used to determine H_0 by the force balance loop. For the EHL case, the same method can be used. However, if L_2 can be put in the system equation and be solved simultaneously without creating a computer memory problem, the computation will be greatly reduced.

The system equation for Newton's method can be written as

$$\begin{pmatrix} [A] & \{B\} \\ \{C\}^T & 0 \end{pmatrix}\begin{pmatrix} \{\delta u\} \\ \delta H_0 \end{pmatrix} = -\begin{pmatrix} \{L_1\} \\ L_2 \end{pmatrix} \tag{20}$$

$$\{u\}^{n+1} = \{u\}^n + \{\delta u\} \tag{21}$$

$$H_0^{n+1} = H_0^n + \delta H_0 \tag{22}$$

where

$$\{u\} = \{P_{I,J}, \hat{G}_J\},\ I = 2,\ NI - 1;\ J = 1,\ NJ - 1$$

and $[A]$, $\{B\}$, $\{C\}^T$ are the elements in the Jacobian matrix.

In EHL, due to the integral operator D, [A] is full matrix. But, since large amounts of storage and computational time are required to solve it, the block tridiagonal matrix approximation can be used. Each block matrix is a full matrix which is different from the one-sided arrow shape matrix that resulted from the

hydrodynamic case where the elasticity equation is not needed. The unknown $\hat{G}$ matches the residual function at the cavitation boundary where the pressures are known from the Reynolds boundary condition.

Equation (20) can be rearranged as

$$[A]\{\delta u\} + \{B\}\delta H_0 = -\{L_1\} \tag{23}$$

$$\{C\}^T\{\delta u\} = L_2 \tag{24}$$

From equation (23)

$$\{\delta u\} = -[A]^{-1}\{L_1\} - [A]^{-1}\{B\}\delta H_0 \tag{25}$$

Then using equations (24) and (25)

$$\delta H_0 = \frac{L_2 - \{C\}^T[A]^{-1}\{L_1\}}{\{C\}^T[A]^{-1}\{B\}} \tag{26}$$

And $\{\delta u\}$ can be calculated using equations (25) and (26). In equation (26), $[A]^{-1}\{B\}$ and $[A]^{-1}\{L_1\}$ are obtained by the Thomas algorithm and then stored temporarily and used in equation (25).

The convergence criteria are

(1) Pressure

$$\frac{\sum_I \sum_J \left| P^{i+1}_{I,J} - P^{n}_{I,J} \right|}{\sum_I \sum_J P^{n}_{I,j}} < 5.0\text{x}10^{-3}$$

(2) Cavitation boundary

$$\frac{\sum_J \left| \hat{G}^{n+i}_J - \hat{G}^{n}_J \right|}{\sum_J \hat{G}^{n}_J} < 5.0\text{x}10^{-3}$$

(3) Reference film thickness

$$\frac{\left| H_0^{n+1} - H_0^{n} \right|}{H_0^{n}} < 5.0\text{x}10^{-3}$$

4. RESULTS AND DISCUSSION

The dimensionless material parameter used in this analysis is G = 3488 in which z = 0.55, μ_0 = 0.018 Ns/m^2, ν = 0.3 and E' = 2.19x10^{-11} N/m^2. In figures 2 and 3, the pressure distribution and film thickness profile for the circular contact is presented. The inlet boundary used for this analysis is defined as X_A = -4.0 and Y_B = 2.0. The maximum pressure is 1.33 times the maximum Hertzian pressure or 515 MPa which occurs on the x-axis. The dimensionless minimum film thickness is 0.27 and it occurs at the side-lobes, X = 0.49 and Y = 0.6.

The majority of the computation time is used for the calculation of the elastic deformations and the differentiations of the residual functions with respect to the cavitation boundary function since the integral operator is a function of it. It takes about 20 sec on the CRAY-XMP at NASA Lewis Research Center for 1 Newton iteration with 3060 nodal points of the whole domain, and, in general, the converged solution can be obtained within 3 iterations as long as the initial guess is within the sphere of attraction. It was reported (ref. 3) that using the multigrid interative method it took 2 hr of CPU time on a VAX11/750 with 2937 nodal points. Since a different computer was used, a direct comparison is difficult. The current method is quite fast partly because the direct matrix inversion of the block matrices is vertorizable which makes it well suited to the supercomputing. Also because the amount of visits to the elasticity subroutine is small and there is no need of a force balance loop. When the current work is used for transient calculations, the previous solution is used as a guess to the next time step and it accelerate the solution process, but this is not true for the iterative method. This fact supports the current work as a good candidate for transient EHL point contact computation.

The calculated minimum film thickness in this investigation for various operating parameters are provided in table I along with those obtained from the H.D. Formula, equation 1. In general, the results from this analysis were higher than those predicted by the H.D. for the circular contact case. However, for the elliptical contact our results were lower. But the differences do not exceed 10 percent.

Figure 4 shows another pressure distribution for circular contact where a very steep pressure spike occurs. The operating condition is $W = 9.154 \times 10^{-8}$, $U = 1.62 \times 10^{-11}$, or $\bar{\alpha} = 5.723$ and $\lambda = 0.862$. The maximum pressure is 2.89 times the maximum Hertzian pressure or 1.04 GPa. To the authors' experience, the solution is so unstable beyond this operation range that the convergence usually fails. When $U = 6.432 \times 10^{-12}$, the maximum possible W is 2.367×10^{-7} for circular contact, or $\bar{\alpha} = 7.862$ and $\lambda = 0.0964$. According to numerous computations, it is found that the value of $\bar{\alpha}$ dictates the numerical stability of current method. The numerical stability may be enhanced by reducing the step sizes near the pressure spike region. But it should be noticed that the Roelands viscosity-pressure relation is known to be valid up to 1 GPa or lower. At such a high pressure the lubricant behaves as a solid-like material and becomes non-Newtonian. Also, recently, it was observed that slippage of the lubricant occurs at or very near the surface (ref. 16). Thus it is believed that the modification of the classical Reynolds equation including the non-Newtonian effect and a more realistic pressure-viscosity relation including the thermal effect are needed to investigate the lubrication performance for the high load and high speed cases.

Figure 5 depicts the calculated free boundaries of the circular contacts for various operating parameters. The x-axis is somewhat stretched to exaggerate the differences. The dotted line represents the Hertzian circle. The general trend is that, as expected, the low speed condition results in a curve that conforms more to Hertzian (dry) contact circle. Comparing curves 1 and 2, the boundary on the X-axis stretches more outside for the higher load but elsewhere it is closer to the Hertzian contact circle. Comparing curves 3 and 4, increasing the speed parameter leads to a thicker film and tends to straighten out the boundary.

5. CONCLUSIONS

The classical EHL point contact problem is solved using a new "system-approach," similar to that introduced by Houpert and Hamrock for the line-contact problem. This

requires inverting a system-matrix (i.e., the Jacobian) which via a body-fitted coordinate transformation includes boundary conditions at the free boundary. Further, a force-balance loop is avoided. Using a Newton-Raphson algorithm, the pressures, the cavitation boundary curve, and the reference film thickness are found simultaneously. The method is computationally fast and has no problem with locating the cavitation boundary. This study revealed that

1. The minimum film thickness obtained in this study were all within 10 percent of the predictions using the H.D. Formula.

2. The algorithm is well suited to performing transient EHL calculations using the supercomputer and the solution at each time step accelerates the succeeding solution.

3. Numerical instabilities were encountered when the value of $\bar{\alpha}$, that is, W or C is high. To obtain a more stable solution, it is believed that the Reynolds equation should be modified to include the non-Newtonian effect and a more realistic pressure-viscosity relation for high pressure.

4. The calculated cavitation boundary is near the Hertzian contact circle but deviates it for high speed.

ACKNOWLEDGEMENT

A part of this work was accomplished while S.G. Lim was a Research Associate in the Department of Engineering, Case Western Reserve University and part as a National Research Council-NASA Lewis Research Associateship.

APPENDIX - DISCRETIZATION ON THE TRANSFORMED REYNOLDS EQUATION FOR k = 1.

$$(L_1)_{I,J} = \left(R_1 + \xi_{I+1/2}R_7\right)\frac{q_{I+1/2,J}}{r_\xi}(P_{I+1,J} - P_{I,J}) - \left(R_1 + \xi_{I-1/2}R_7\right)q_{I-1/2,J}(P_{I,J} - P_{I-1,J})$$

$$+ R_2\left(\frac{q_{I,J+1/2}}{r_\eta}(P_{I,J+1} - P_{I,J}) - q_{I,J-1/2}(P_{I,J} - P_{I,J-1})\right) - R_3\left(R_4 q_{I,J+1/2}DP_1 - R_5 q_{I,J-1/2}DP_2\right)$$

$$- R_6\left(q_{I+1/2,J}DP_3 - q_{I-1/2,J}DP_4\right) - R_8\left(\bar{\rho}_{I+1/2,J}H_{I+1/2,J} - \bar{\rho}_{I-1/2,J}H_{I-1/2,J}\right) = 0$$

where,

$$R_1 = \frac{2Y_B^2}{(\hat{G}_J - X_A)^2(1 + r_\xi)\Delta\xi^2}$$

$$R_2 = \frac{2}{(1 + r_\eta)\Delta\eta^2}$$

$$R_3 = \frac{\xi_I}{r_\xi(1 + r_\xi)(1 + r_\eta)\Delta\xi\Delta\eta}$$

$$R_4 = \frac{\hat{G}'_{J+1/2}}{\hat{G}_{J+1/2} - X_A}$$

$$R_5 = \frac{\hat{G}'_{J-1/2}}{\hat{G}_{J-1/2} - X_A}$$

$$R_6 = \frac{\xi_I\hat{G}'_J}{(G_J' - X_A)r_\eta(1 + r_\xi)(1 + r_\eta)\Delta\xi\Delta\eta}$$

$$R_7 = \frac{2\xi_I(\hat{G}'_J)^2}{(1 + r_\xi)\Delta\xi^2(\hat{G}_J - X_A)^2}$$

$$R_8 = \frac{2\lambda Y_B}{(\hat{G}_J - X_A)\Delta\xi(1+r_\xi)}$$

$$\Delta\xi = \xi_I - \xi_{I-1}$$

$$r_\xi\Delta\xi = \xi_{I+1} - \xi_I$$

$$\Delta\eta = \eta_J - \eta_{J-1}$$

$$r_\eta\Delta_\eta = \eta_{J+1} - \eta_J$$

$$DP_1 = -r_\xi^2(P_{I-1,J} + P_{I-1,J+1}) + (r_\xi^2 - 1)(P_{I,J} + P_{I,J+1}) + (P_{I+1,J} + P_{I+1,J+1})$$

$$q_{I,J} = \frac{\overline{\rho}_{I,J} H^3_{I,J}}{\overline{\mu}_{I,J}}$$

$$DP_2 = -r_\xi^2 (P_{I-1,J} + P_{I-1,J-1}) + (r_\xi^2 - 1)(P_{I,J} + P_{I,J-1}) + (P_{I-1,J} + P_{I+1,J-1})$$

$$DP_3 = -r_\eta^2 (P_{I,J-1} + P_{I+1,J-1}) + (r_\eta^2 - 1)(P_{I,J} + P_{I+1,J}) + (P_{I,J+1} + P_{I+1,I+1})$$

$$DP_4 = -r_\eta^2 (P_{I,J-1} + P_{I-1,J-1}) + (r_\eta^2 - 1)(P_{I,J} + P_{I-1,J}) + (P_{I,J+1} + P_{I-1,J+1})$$

REFERENCES

1. Hamrock, B.J. and Dowson, D., "Isothermal Elastohydrodynamic Lubrication of Point Contacts, Part III, Fully Flooded Results," J. Lubr. Technol., 99, pp. 264-276 (1977).

2. Cryer, C.W., "The Method of Christopherson for Solving Free Boundary Problems for Infinite Journal Bearings by Means of Finite Differences," Math. Comput., 25, pp. 435-443 (1971).

3. Lubrecht, A.A., Ten Napel, W.E., And Bosma, R., "Multigrid, and Alternative Method of Solution for Two-Dimensional Elastohydrodynamically Lubricated Point Contact Calculations," J. Tribology, 109, pp. 437-443 (1987).

4. Oh, K.P., "The Numerical Solution of Dynamically Loaded Elastohydrodynamic Contact as a Nonlinear Complementarity Problem," J. Tribology, 106, pp. 88-95 (1984).

5. Cryer, C.W., "The Solution of a Quadratic Programming Problem Using Systematic Overrelaxation," SIAM J. Control, 9, pp. 385-392 (1984).

6. Kostreva, M.M., "Elastohydrodynamic Lubrication: A Nonlinear Complementarity Problem," Int. J. Numer. Meth. Fluids, 4, pp. 377-397 (1984).

7. Oh, K.P. and Rohde, S.M., "Numerical Solution of the Point Contact Problem Using the Finite Element Method," Int. J. Numer. Methods Eng., 11, pp. 1507-1518 (1977).

8. Houpert, L.G. and Hamrock, B.J., "Fast Approach for Calculating Film Thicknesses and Pressures in the Elastohydrodynamically Lubricated Contacts at High Loads," J. Tribology, 108, pp. 411-420 (1986).

9. Okamura, H., "A Contribution to the Numerical Analysis of Isothermal Elastohydrodynamic Lubrication," Tribology of Reciprocating Engines, Proceedings of the 9th Leeds-Lyon Symposium on Tribology, Butterworths, Guilford, England, pp. 313-320 (1982).

10. Crank, J., Free and Moving Boundary Problems, Claredon Press, (1984).

11. Roelands, C.J.A., Ph.D. Dissertation, University of Delft, (1966).

12. Dowson, D. and Higginson, G.R., Elasto-hydrodynamic Lubrication, Pergamon, Oxford (1966).

13. Lim, S.G., Brewe, D.E., and Prahl, J.M., "On the Numerical Solution of the Dynamically Loaded Hydrodynamic Lubrication of the A Point Contact Problem," NASA TM-102427 (1990).

14. Chang, L., "An Efficient and Accurate Formulation of the Surface-Deflection Matrix in Elastohydrodynamic Point Contacts," J. Tribology, 111, pp. 642-647 (1989).

15. Vinokur, M., "On One-Dimensional Stretching Functions for Finite-Difference Calculations," J. Comput. Phys., 50, pp. 215-234 (1983).

16. Kaneta, M., Nishikawa, H., And Kameishi, K., "Obervation of Wall Slip in Elastohydrodynamic Lubrication," J. Tribology, 112, pp. 447-452 (1990).

17. Evans, C.R. and Johnson, K.L., "The Rheological Properties of Elastohydrodynamic Lubricants," Proc. Inst. Mech. Eng. Pt.C Mech. Eng. Sci., 200, pp. 303-312 (1986).

18. Kostreva, M.M., "Pressure Spikes and Stability Considerations in Elastohydrodynamic Lubrication Models," J. Tribology, 106, pp. 386-395 (1984).

TABLE I. - SELECTED MINIMUM FILM THICKNESS

r	k	$U \times 10^{12}$	$W \times 10^{8}$	H_{min}	H_{min}	$\frac{H_{min} - H_{min}H.B.}{H_{min}} \times 100$
1.0	1.0	6.432	6.721	0.398	0.369	7.3
1.0	1.0	6.432	11.227	0.270	0.252	6.7
1.0	1.0	7.968	5.566	0.525	0.490	6.7
1.0	1.0	16.204	5.566	0.798	0.794	0.5
6.0	3.25	6.432	13.700	0.729	0.763	-4.7
6.0	3.25	6.432	27.464	0.433	0.456	-2.9
16.0	6.037	6.432	32.707	0.626	0.654	-4.5

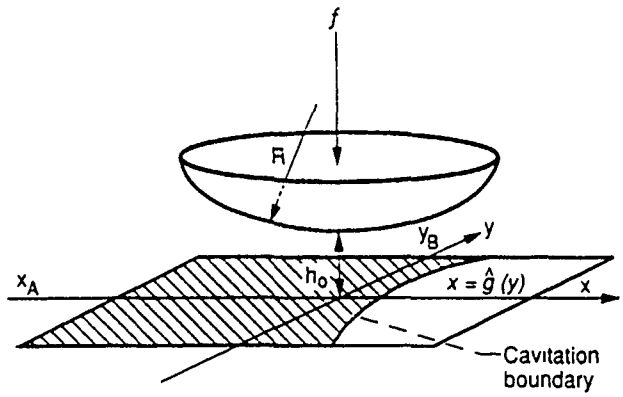

Figure 1.—Point contact EHL model.

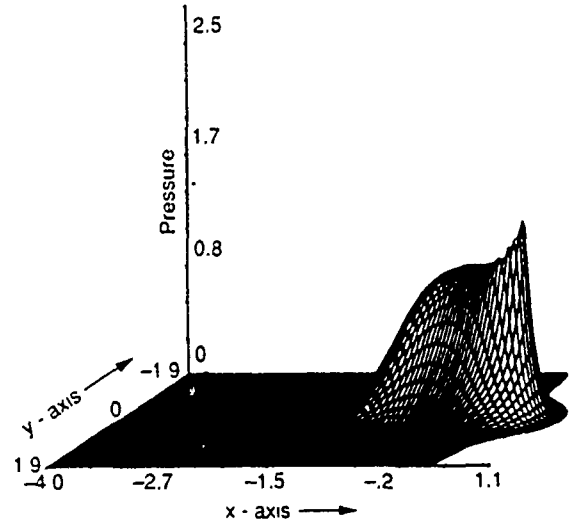

Figure 2.—Pressure distribution for $W = 1.123 \times 10^{-7}$, $U = 6.432 \times 10^{-12}$, G = 3488, and k = 1.

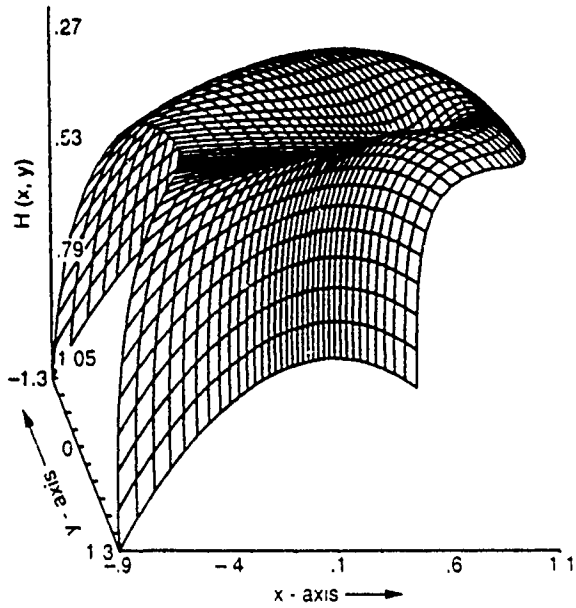

Figure 3. —Film thickness profile near contact for parameters in Figure 2.

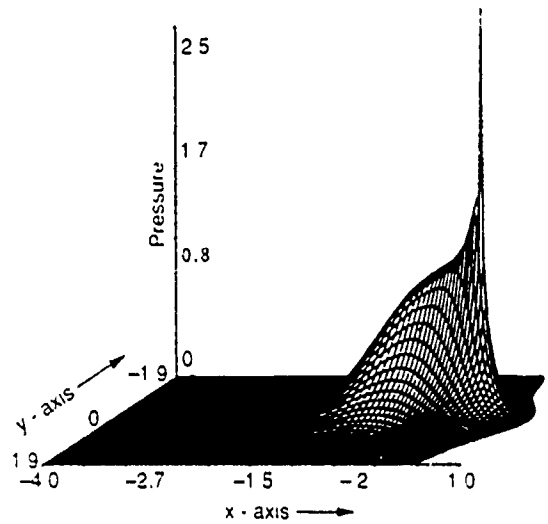

Figure 4 —Pressure distribution for $W = 9\ 154 \times 10^{-8}$, $U = 1.620 \times 10^{-11}$, G = 3488, and k = 1.

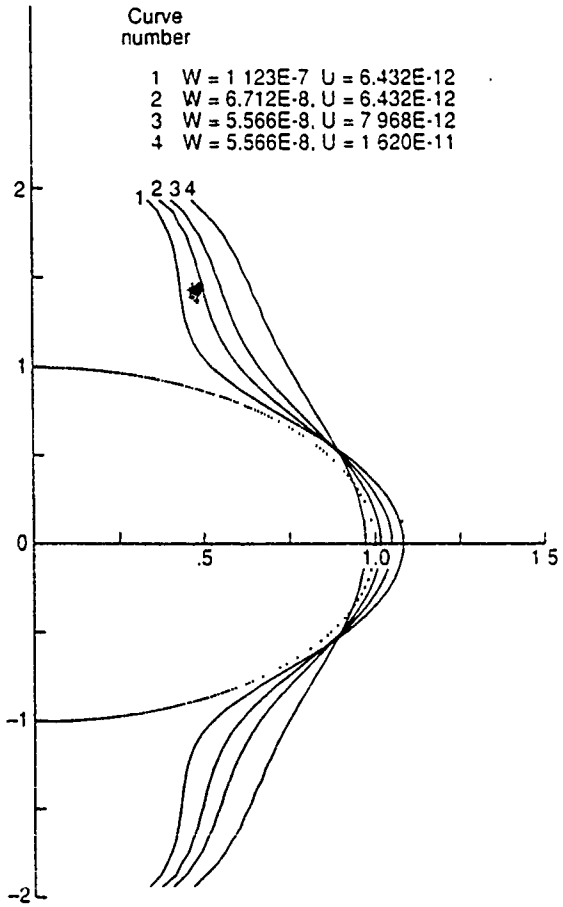

Figure 5 —Calculated cavitation boundaries.

NASA
National Aeronautics and Space Administration

Report Documentation Page

1. Report No.	2. Government Accession No.	3. Recipient's Catalog No.
NASA TM - 104342 AVSCOM TR 90 - C - 031		

4. Title and Subtitle
A System-Approach to the Elastohydrodynamic Lubication Point-Contact Problem

5. Report Date

6. Performing Organization Code

7. Author(s)
Sang Gyu Lim and David E. Brewe

8. Performing Organization Report No.
E-6116

9. Performing Organization Name and Address
NASA Lewis Research Center
Cleveland, Ohio 44135 - 3191
and
Propulsion Directorate
U.S. Army Aviation Systems Command
Cleveland, Ohio 44135 - 3191

10. Work Unit No.
505 - 63 - 5A
1L161102AH45

11. Contract or Grant No.

12. Sponsoring Agency Name and Address
National Aeronautics and Space Administration
Washington, D.C. 20546 - 0001
and
U.S. Army Aviation Systems Command
St. Louis, Mo. 63120 - 1798

13. Type of Report and Period Covered
Technical Memorandum

14. Sponsoring Agency Code

15. Supplementary Notes
Prepared for the Annual Meeting of the Society of Tribologists and Lubrication Engineers, Montreal, Quebec, Canada, April 29—May 2, 1991. Sang Gyu Lim, National Research Council-NASA Research Associate at Lewis Research Center; David E. Brewe, Propulsion Directorate, U.S. Army Aviation Systems Command. Responsible person, David E. Brewe, (216) 433 - 6067.

16. Abstract
The classical EHL point contact problem is solved using a new "system-approach," similar to that introduced by Houpert and Hamrock for the line-contact problem. Introducing a body-fitted coordinate system, the troublesome free-boundary is transformed to a fixed domain. The Newton-Raphson method can then be used to determine the pressure distribution and the cavitation boundary subject to the Reynolds boundary condition. This method provides an efficient and rigorous way of solving the EHL point contact problem with the aid of a supercomputer and a promising method to deal with the transient EHL point contact problem. A typical pressure distribution and film thickness profile are presented and the minimum film thicknesses are compared with the solution of Hamrock and Dowson. The details of the cavitation boundaries for various operating parameters are discussed.

17. Key Words (Suggested by Author(s))	18. Distribution Statement
Elastohydrodynamic; Lubrication; Gears; Transient loads; Numerical analysis; Free boundaries; Pressure distribution; Film thickness	Unclassified - Unlimited Subject Category 34

19. Security Classif. (of the report)	20. Security Classif. (of this page)	21. No. of pages	22. Price*
Unclassified	Unclassified	16	A03

NASA FORM 1626 OCT 86

*For sale by the National Technical Information Service, Springfield, Virginia 22161